

Supporting Information for

Reviving Rechargeable Lithium Metal Batteries: Enabling Next-generation High-energy and High-power Cells

Aruna Zhamu,^{1,2} Guorong Chen,¹ Chenguang Liu,^{1,*} David Neff,¹ Qing Fang¹, Zhenning Yu,²
Wei Xiong,² Yanbo Wang,² Xiqing Wang,¹ and Bor Z. Jang,^{1,*}

¹ Nanotek Instruments, Inc., and ² Angstrom Materials, Inc., 1242 McCook Ave., Dayton, Ohio
45404

* Corresponding Author: Bor.Jang@NanotekInstruments.com or
chenguang.liu@NanotekInstruments.com

Experimental Details

Preparation of Li-Graphene Cells: Oxidized graphene or graphene oxide (GO) was prepared with a modified Hummers' method that involved exposing the starting graphitic materials (natural graphite, artificial graphite, meso-phase carbon, and carbon fibers) to a mixture of sulfuric acid, sodium nitrate, and potassium permanganate at a ratio of 4:1:0.1 for 72 hours. The resulting GO was then thoroughly rinsed with water to obtain GO suspension, which was followed by two different routes of material preparation.

One route involved subjecting the GO suspension to ultrasonication to obtain isolated graphene oxide sheets suspended in water. For Electrode-N, GO was obtained from natural graphite. After drying the ultrasonicated suspension in an aerosolizing oven, the resulting flower-shape aggregates of GO sheets were thermally reduced at 500°C for 2 hours to significantly improve the electrical conductivity.

The other route involved drying GO suspension to obtain graphite intercalation compound (GIC) or GO powder. The GIC or GO powder was then thermally exfoliated at 1,050°C for 45 seconds to obtain exfoliated graphite or graphite worms. Exfoliated graphite (EG) from artificial graphite was used to make an electrode (Electrode-EG). However, exfoliated graphite worms from meso-phase carbon and carbon fibers were subsequently subjected to ultrasonication to separate or isolate oxidized graphene sheets to prepare Electrode-M and Electrode-C, respectively.

Each electrode, composed of 85% graphene, 5% Super-P (acetylene black-based conductive additive), and 10% PTFE, was coated on Al foil for use as a cathode. For use as an extension of an anode current collector, the mixture paste was coated to a sheet of Cu foil. Alternatively, in 4 of the LG-N cells, no copper foil was used, where the graphene layer itself was the current collector. The thickness of the electrode was typically around 150-300 μm, but an additional series of samples with thicknesses of approximately 20-150 μm was prepared to evaluate the effect of electrode size on the power and energy densities of the resulting Li-graphene cells. The electrode was dried in a vacuum oven at 120°C for 12 hours before use. Prelithiation of some graphene layers as a negative electrode was conducted by plating Li metal onto graphene sheet surfaces in an electrochemical cell containing exactly the same electrolyte as utilized in the Li-graphene cells (1M LiPF₆/EC+DMC). Both coin-size and pouch cells were assembled in a glove box with a good control of both moisture and oxygen levels.

Some of the Li-graphene cells investigated are summarized in Table S1 below. In each group, some cells contain a graphene-based anode current collector electrochemically prelithiated (pre-plated) with Li and other cells contain pieces of Li foil mixed with the graphene sheets in the anode. The amount

of graphene is selected to provide an anode specific capacity of 1000-3000 mAh/g based on the total weight of graphene and Li combined.

Table S1 Types of Li-graphene cells subjected to electrochemical testing (including long-term cycling test).

Cell ID	Anode composition	Cathode composition	Gravimetric current density or charge/discharge rate	Comments
LG-N (both pouch and coin cells)	Electrode N (graphene from natural graphite) as an extended anode current collector; prelithiated or with Li foil	N graphene as a cathode active material	From 20 mA/g to 10 A/g for thicker electrodes (> 200 μm); up to 225 A/g for thinner electrodes (20-150 μm)	Li-graphene cell; 12 cells were run for > 2,000 cycles at high rates (1-10 A/g); graphene/Li wt. ratio = 10/1, 1/1, and 1/5
LG-EG (coin cells)	Electrode EG (highly exfoliated graphite worms) as an extended current collector	EG as a cathode active material	From 20 mA/g to 10 A/g	Li-graphene cell: 8 cells were run for > 1000 cycles
LG-M (coin cells)	Electrode M (graphene from meso-carbon) as an extended current collector	M as a cathode active material	From 20 mA/g to 10 A/g	Li-graphene cell: 5 cells were run for > 1000 cycles
LG-C (coin cells)	Electrode C (graphene from carbon fiber) as an extended current collector	C as an active material	From 20 mA/g to 10 A/g	Li-graphene cell: 5 cells were run for > 1000 cycles

The Preparation of Li-Vanadium Oxide Cells: Most of the cathode materials in current lithium-ion batteries exhibit a specific capacity significantly lower than 200 mAh/g (e.g., 150 mAh/g for LiCoO₂). One exception is vanadium-based materials (e.g. Li_xV₂O₅ and Li_{1+x}V₃O₈) that exhibit exceptional specific capacity due to their ability to incorporate more than one lithium ion per vanadium atom. For example, a specific discharge capacity of 442 mAh/g was obtained when three lithium ions intercalate into V₂O₅. Nanometer thick Li_xV₂O₅ nano-belts with the δ-type crystal structure, synthesized by a hydrothermal treatment of Li⁺-exchanged V₂O₅ gel, were found to exhibit a specific capacity of 490 mAh/g. Lithium trivanadate (Li_{1+x}V₃O₈) is another vanadium oxide that also can accommodate several lithium ions per formula.

In the present investigation, the synthesis of LiV₃O₈ nano-belts involves mixing equivalent amounts of LiOH and V₂O₅ powder in distilled water under stirring, and keeping the reactor in a water bath at 50°C for 24h. The yellow color of the initial mixture solution turned into a red-brown gel indicating the formation of the LiV₃O₈. A suspension of 1% by weight graphene oxide (GO) in water was then poured into the LiV₃O₈ gel. The mixture suspension was cooled to room temperature and poured into liquid nitrogen to undergo freeze-drying. Finally, the dried LiV₃O₈ precursor was heat-treated in Ar at 300°C for 8h to thoroughly remove water to recover NLV cathode. A baseline cathode (LV) without graphene was prepared under comparable conditions as used in NLV, but without the utilization of GO during processing. Representative SEM images of LV and NLV are given in Fig. 3A and 3B of the manuscript. It is clear that essentially all of the LiV₃O₈ nano-belts or nano-sheets are enclosed by graphene sheets into substantially spherical or ellipsoidal particles. These regular-shape morphologies facilitate close packing (having good packing density) when the particles are made into an electrode. The embracing graphene sheets also serve to prevent direct contact of LiV₃O₈ with electrolyte, significantly

curtailing the possibility of LiV_3O_8 getting dissolved in liquid electrolyte (a major capacity decaying mechanism associated with a LiV_3O_8 -based cell).

Two groups of Li-vanadium oxide cells (Table S2) were prepared and tested for the possibility of observing dendrites at the Li metal anode. Both pouch cells and button cells were investigated. In each group, some cells contain a graphene-based anode current collector prelithiated with Li, but other cells contain pieces of Li foil mixed with the graphene sheets in the anode. The amount of graphene is selected to provide an anode specific capacity of 1000-3000 mAh/g based on the total weight of graphene and Li combined.

For the purpose of comparing the specific capacity and energy density of both Li-graphene and Li-Vanadium Oxide cells against those of conventional Li-ion cells, we fabricated pouch cells of approximately the same dimensions as the conventional PL-383450 graphite- LiCoO_2 cell (Table S3).

Table S2 Types of Li-vanadium oxide cells subjected to electrochemical testing (including long-term cycling test).

Cell ID	Anode composition	Cathode composition	Current density or charge/discharge rate	Comments
Li-NLV (both pouch and coin cells)	Electrode N (graphene from natural graphite) as an extended anode current collector; 2 cells with a prelithiated anode and 2 with stips of Li foil	Graphene-embraced LiV_3O_8 nano-belts (5% by weight graphene)	0.5 C, 2.5 C, and 10 C rates	6 cells were stopped for inspection after 300 cycles; 6 cells after 500 cycles; no cell failure and no dendrite observed
Li-LV (coin cells)	Electrode N (graphene from natural graphite) as an extended anode current collector; 2 cells with a prelithiated anode and 2 with stips of Li foil	LiV_3O_8 nano-belts without graphene	0.5 C and 2.5 C rates	2 cells were run for 300 cycles and 2 for 500 cycles; no cell failure, but with significant capacity decay; cells stopped for dendrite examination; no dendrite observed

Table S3 Actual cell dimensions, weights, capacity rating, and energy density of three types of cells fabricated in our laboratory. The specific capacity and energy density are calculated with or without counting the Cu foil weight since highly conductive graphene can act as a current collector without Cu foil. The Li-graphene cell herein listed is based on a graphene cathode with a specific capacity of 350 mAh/g.

Pouch cells (PL-383450)			w/o Cu foil	w/o Cu foil	w/Cu foil	w/Cu foil
Component	Conventional Li-ion cell (Graphite-LiCoO ₂)		Li-Graphene Cell	Li-VO Cell	Li-Graphene Cell	Li-VO Cell
	Weight (g)	Sizes (mm), w x L x h	Weight (g)	Weight (g)	Weight (g)	Weight (g)
Cathode	5.85	42 x 320	5.85	5.85	5.85	5.85
Anode	2.4	42.5 x 325	0.6	0.5	0.6	0.5
Separator	0.89	44.5 x 700 x 0.025	0.89	0.89	0.89	0.89
Electrolyte	2.56		2.56	2.56	2.56	2.56
Al foil	0.65	42 x 320 x 0.015	0.65	0.65	0.65	0.65
Cu foil	1.4	42.5x325x0.01	0	0	1.4	1.4
Packing	0.67	73x 51 x 0.1	0.67	0.67	0.67	0.67
Tabs	0.13		0.13	0.13	0.13	0.13
Total wt.	14.55		11.05	11.05	12.45	12.45
Design capacity (mAh)	700		1750	1500	1750	1500
Cell specific capacity (mAh/g)	48.11		154.2	133.3	137.2	118.6
Specific energy (Wh/kg)	168.4		462.6	346.7	411.6	308.3

Testing and Characterization: The capacity was measured with galvanostatic experiments using an Arbin SCTS electrochemical testing instrument. Cyclic voltammetry (CV) was conducted on a CHI 660 Instruments electrochemical workstation. Scanning electron microscopy (SEM, Hitachi S-4800), transmission electron microscopy (TEM, Hitachi H-7600), FTIR (PerkinElmer GX FT-IR), Raman spectroscopy (Renishaw inVia Reflex Micro-Raman), and atomic force microscopy were used to characterize the chemical compositions and microstructure of the graphene and exfoliated graphite samples.

Calculations

Galvanostatic charge/discharge tests were used to evaluate electrochemical performance of various Li-graphene cells. The results obtained are expressed as capacity, energy, and power per unit mass of the cell weight (total weights of electrodes, separator, electrolyte, packaging pouch, terminal taps, and current collectors combined) for all pouch cells. For the coin cells with very thin electrodes (< 200 μm), it would have been improper to use the total cell weight by simply adding all the experimental component weights together since the same current collectors used

for thicker electrodes would occupy weights that are out-of-proportion (with respect to the active material amounts). In these cases, the total cell weight is obtained by multiplying the cathode weight with a factor of 2.5 for the purpose of calculating the specific capacity, energy density, and power density.

For the galvanostatic tests of Li-graphene cells, the specific capacity (q) is calculated according to: $q = I * t / m$ (S1)

where I is the constant current in mA, t is the time in hours, and m is the cell mass in grams as defined above. With voltage V , the specific energy (E) is calculated as: $E = \int Vdq$ (S2)

The specific power (P) can be calculated as: $P = E / t$ (S3)

where t is the total charge or discharge step time.

The specific capacitance (C) of the Li-graphene cell, if treated like a supercapacitor cell, is represented by the slope at each point of the voltage- vs.-specific capacity plot.

For the Li-vanadium oxide cells, all the specific capacity, energy density, and power density data were obtained directly from our battery cycling testers (totally 200 cell testing channels are available in our laboratory).

Electrochemical Behaviors

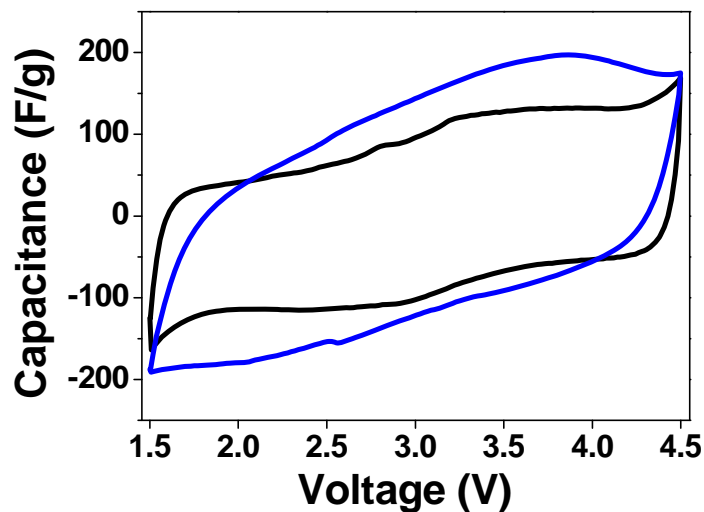
The cyclic voltammetry (CV) diagrams and galvanostatic charge/discharge curves of some Li-graphene cells are in Fig. S1A and S1B, respectively. Only relatively weak redox peaks were observed in the CV curves. It may be noted that the CV curves of both the conventional pseudo-supercapacitors and lithium-ion batteries tend to exhibit a strong redox peak due to slower Faradaic redox reactions taking place in the bulk of an electrode active material (e.g., polyaniline in a pseudo-capacitor, lithium titanate in a lithium-ion battery, and $\text{Li}_x\text{C}_6\text{O}_6$ in an organic electrode battery). The lack of a strong, well-defined redox reaction peak in the CVs of the Li-graphene cells might be simply due to the relatively fast and low-barrier reaction between surface functional groups and ultra-small lithium ions, or fast adsorption of Li ions onto benzene ring centers of graphene sheets¹⁻⁴.

Several observations can be made from Fig. 2C (Ragone plot) of the manuscript:

- (1) The Li-graphene cells can exhibit a high energy density of 320 Wh/kg_{cell}, significantly greater than that of a lithium-ion battery¹.
- (2) A power density as high as 187 kW/kg_{cell} was achieved concurrently with an energy density of 24 Wh/kg_{cell}. This power density is one order of magnitude higher than that of conventional supercapacitors that have the noted capability of delivering a high power density, but with a shortcoming of storing a low energy density of 5 Wh/kg_{cell}.
- (3) This exceptional power density of 187 kW/kg_{cell} is 2-3 orders of magnitude higher than those (typically 0.1-1.0 kW/kg_{cell}) of conventional lithium-ion batteries.
- (4) In the intermediate range between the highest energy density and highest power density, for instance, a Li-graphene cell can maintain an energy density value over 100 Wh/kg_{cell}, while also delivering a power density of 18 kW/kg_{cell}. In contrast, the power density of commercial activated carbon-based symmetric supercapacitors is typically in the range of 1-10 kW/kg_{cell} at an energy density of 5 Wh/kg_{cell}. This implies that, compared with a conventional supercapacitor at the same power density, the Li-graphene cells can deliver > 20 times the energy density.

(5) These data have clearly demonstrated that the Li-graphene cells are a class of energy storage cells by itself, distinct from both conventional supercapacitors and lithium-ion batteries. The cycling performance for a Li-graphene cell is shown in Fig. 3E.

a



b

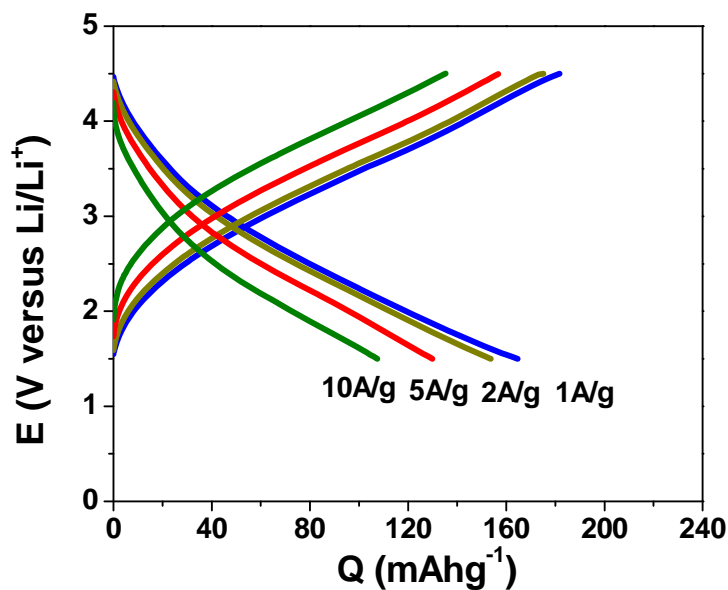
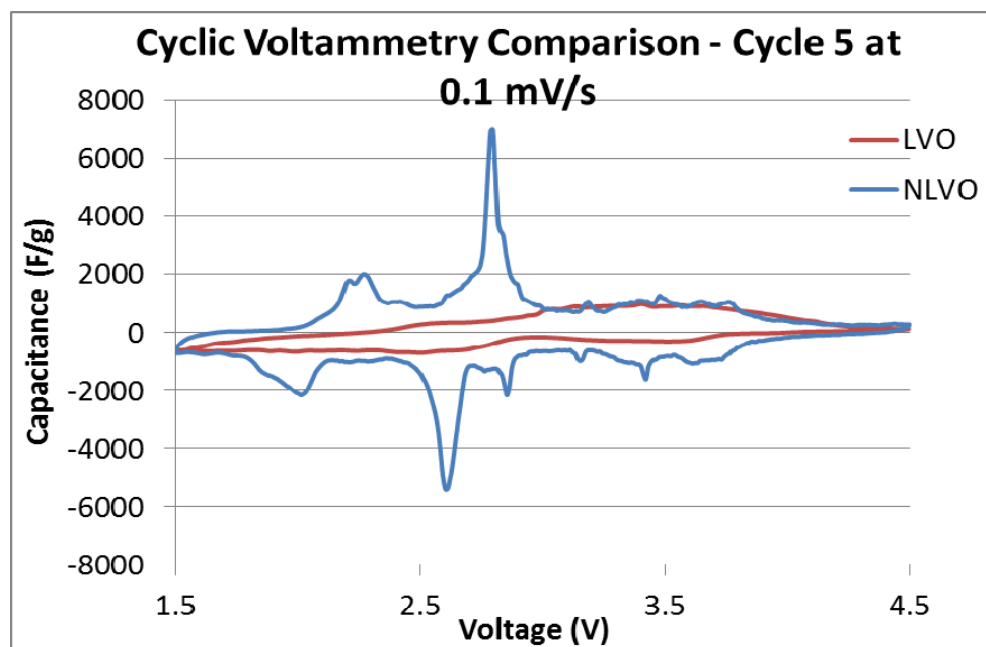


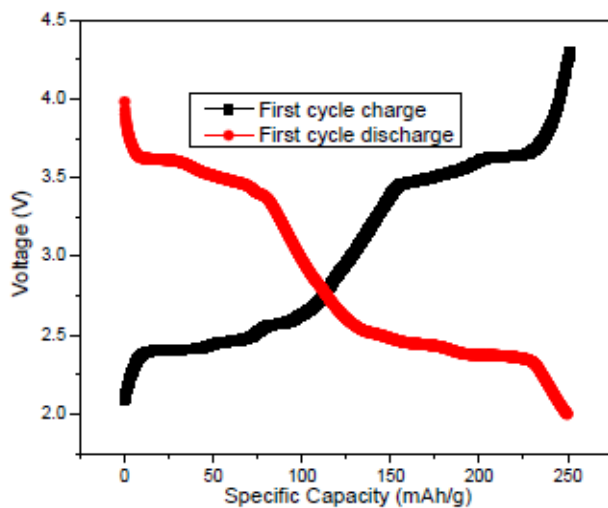
Figure S1 a, Representative CV curves of a reduced graphene oxide (GO) based Li-graphene cell after 50 cycles (black) and a non-reduced GO-based Li-graphene cell (blue). No significant redox peak was observed. The scan rate is 25 mV/s. Electrolyte is 1 M LiPF₆/EC+DMC. **b**, Charge/discharge curves of a non-reduced GO-based Li-graphene cell over a voltage range of 1.5-4.5 volts¹.

Representative CV diagrams and charge-discharge curves of Li-vanadium oxide cells are presented in Fig. S2.

a



b



c

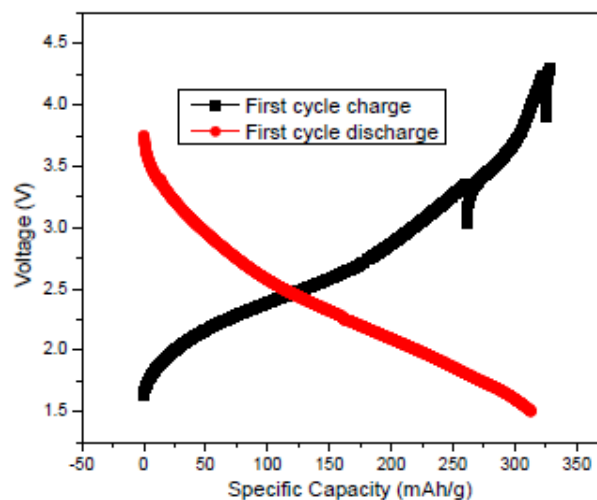
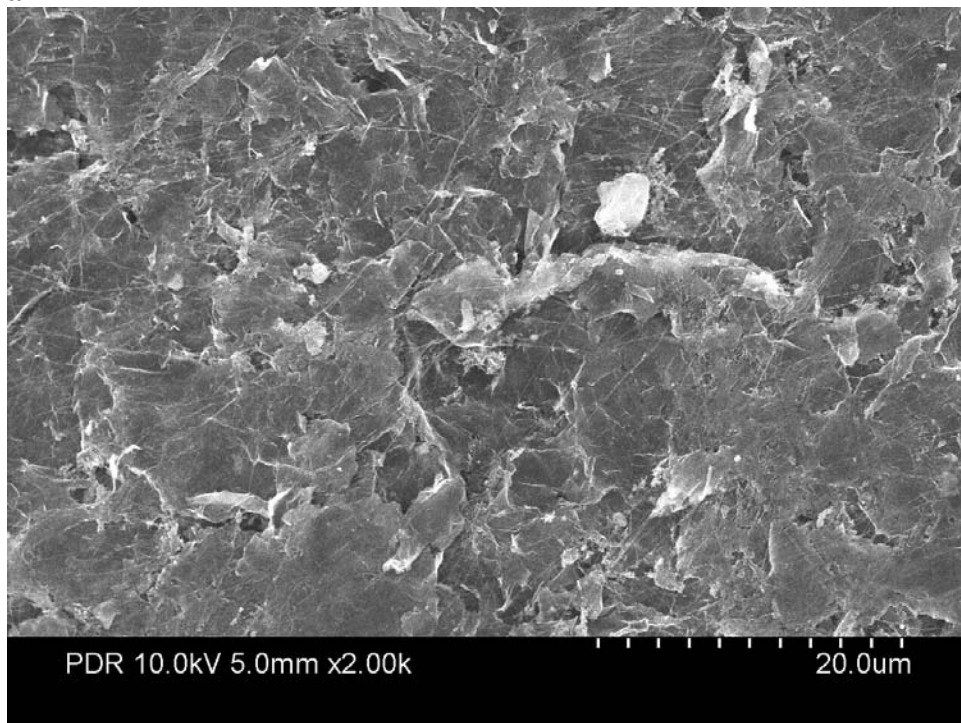


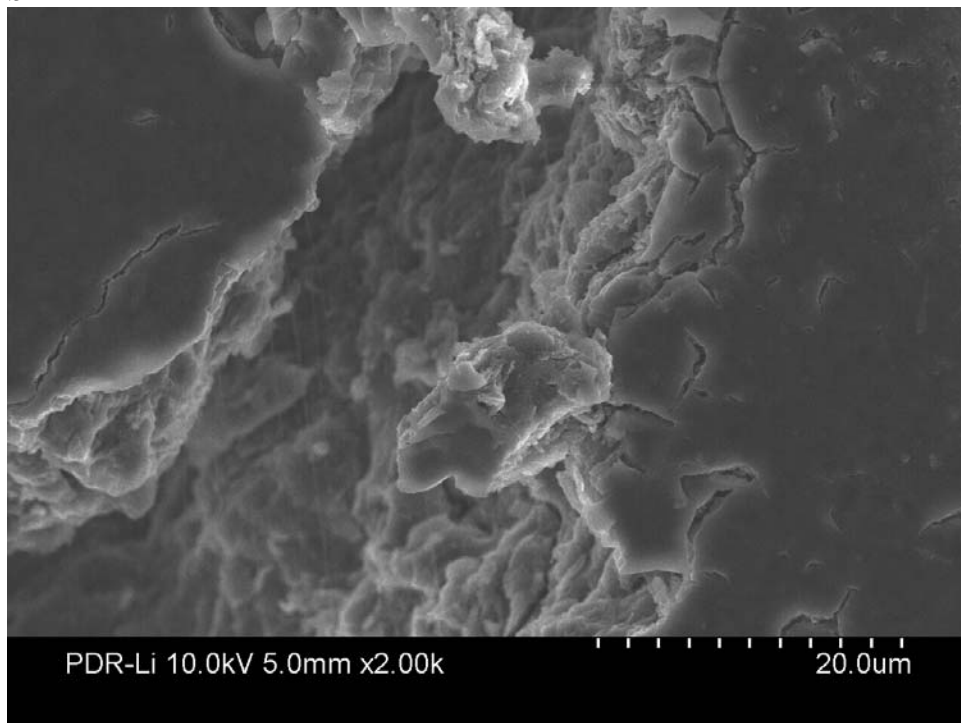
Figure S2 a, CV curves of Li-vanadium oxide cells after 5 cycles (red, LVO) and a corresponding cell with secondary particles of graphene-embraced vanadium oxide as a cathode active material (blue, NLVO). The scan rate is 0.1 mV/s. **b**, Charge/discharge curves of a NLVO cell. **c**, Charge/discharge curves of another NLVO cell. All values were calculated based on the total cathode weight (cathode active material + conductive additive/graphene + binder).

The SEM images of various graphene anode (current collectors), before and after cycling, are presented in Fig. S3 below:

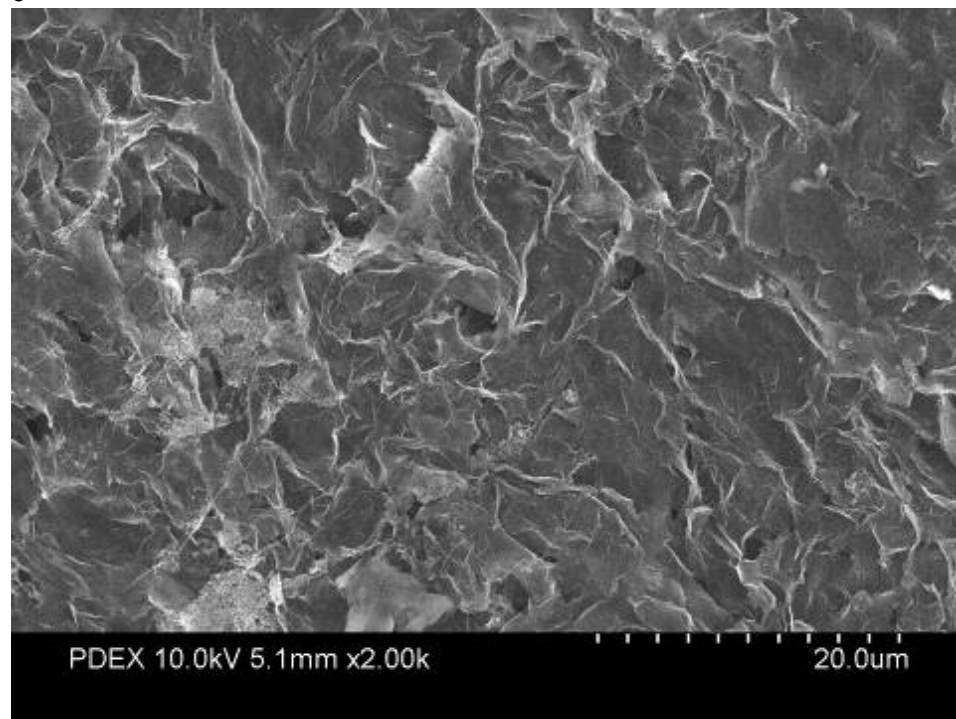
a



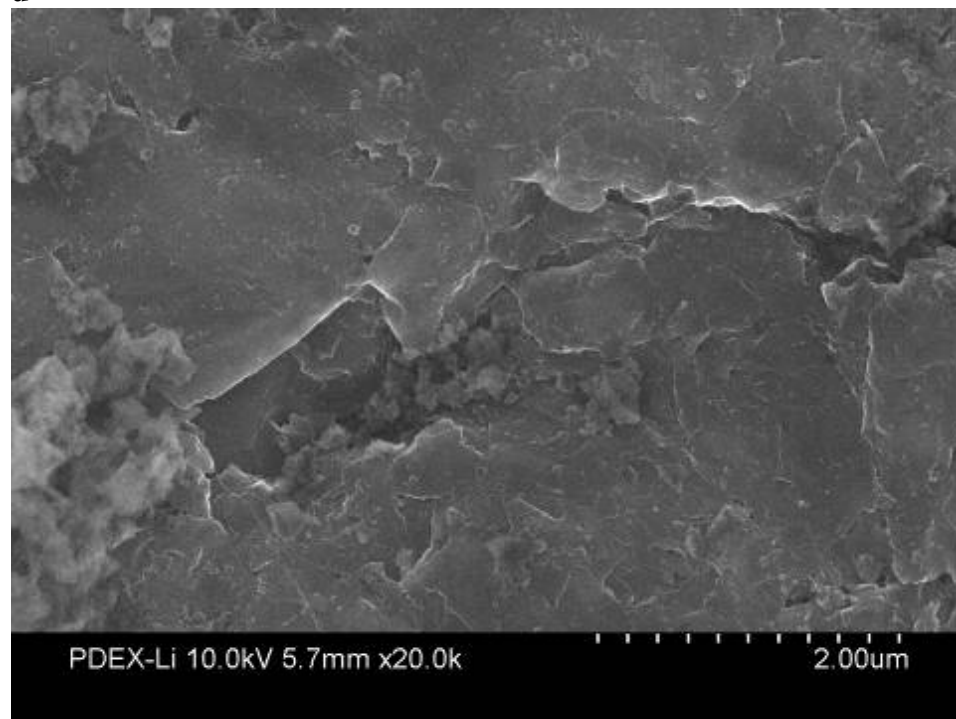
b



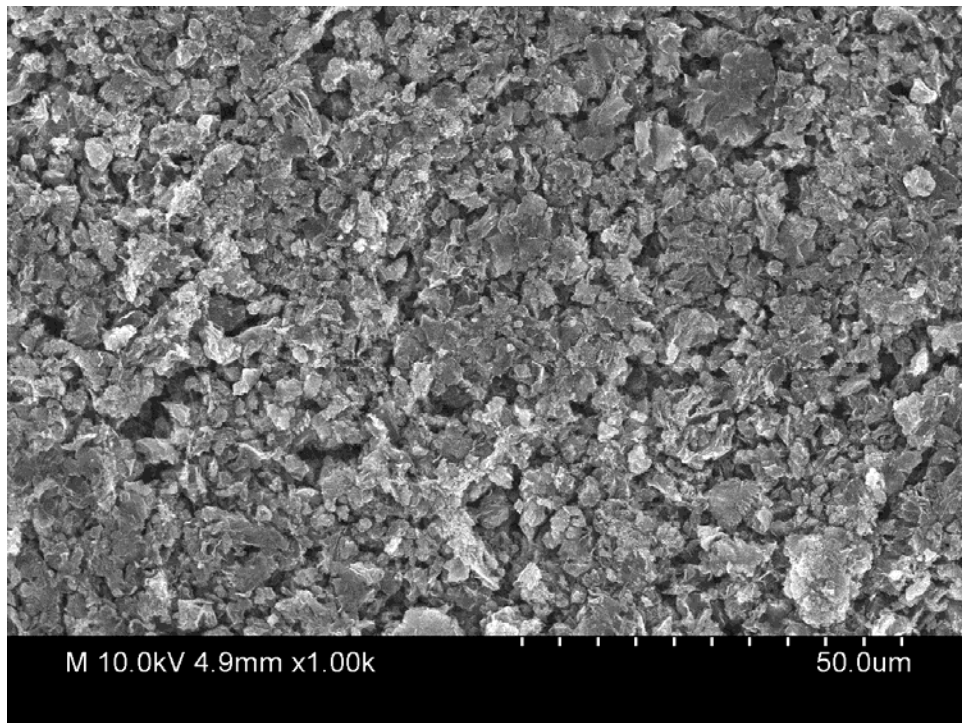
c



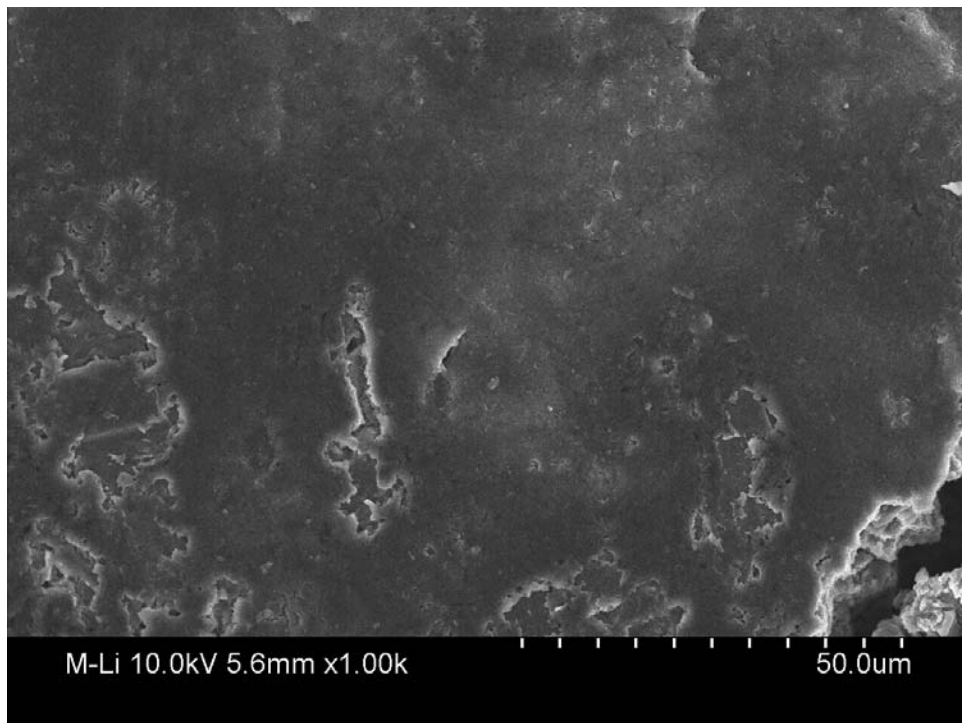
d



e



f



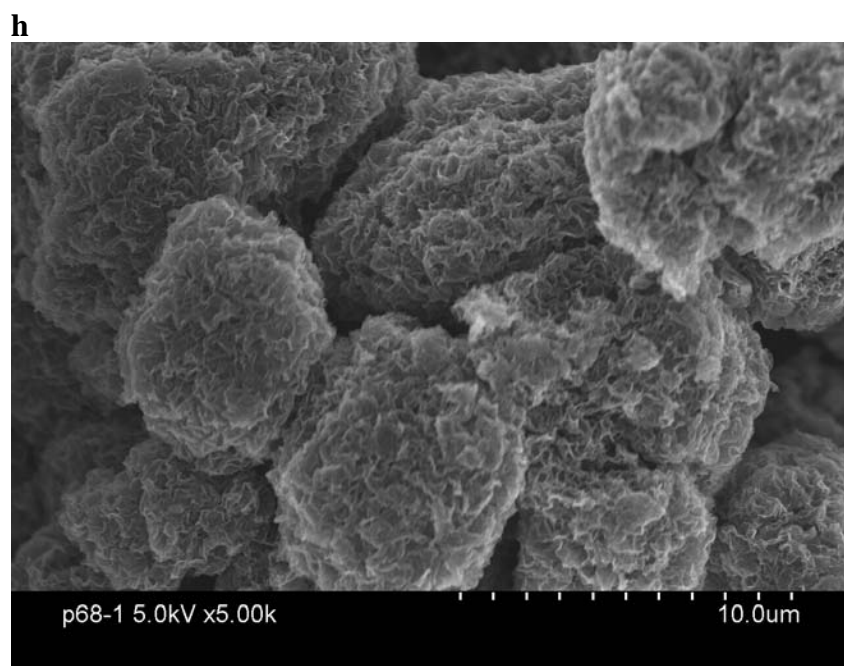
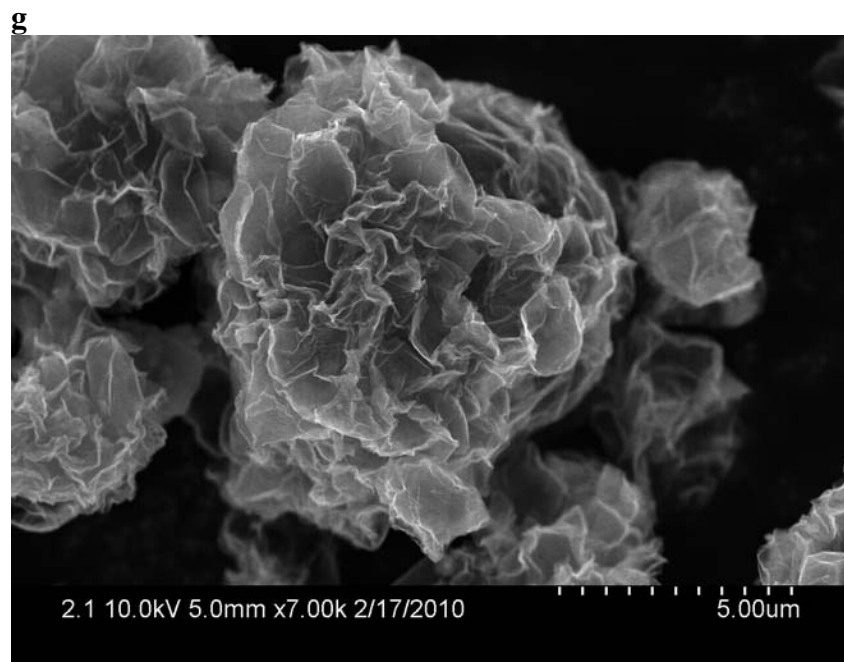


Figure S3 SEM images of graphene-based anode current collectors before and after repeated replating: **a**, and **b**, for reduced graphene oxide-based electrode. **c**, and **d**, for highly thermally exfoliated graphite electrode. **e**, and **f**, for electrode M (graphene from meso-phase carbon). **g**, and **h**, for one type of electrode N (flower-shape graphene from natural graphite).

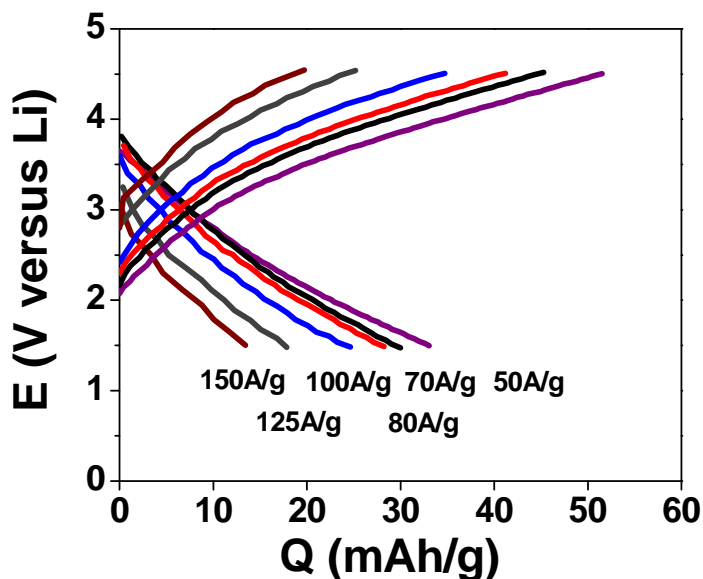


Figure S4 Charge-discharge curves of select Li-graphene cells.

Preliminary Thoughts about Li ion-Capturing Mechanisms at the Cathode of a Li-Graphene Cell

One plausible mechanism (Mechanism 1) is the rapid formation of a surface redox pair between a lithium ion and a carbonyl group, a mechanism proposed and confirmed earlier by others for organic and CNT electrodes²⁻⁴. Mechanism 2 is based on conventional electric double layers of charges formed by cations and anions, which is found to provide typically between 5 and 20% of the total energy in the cell. The lack of a strong or well-defined redox reaction peak in the CVs of chemically reduced graphene oxide (Fig. 3A) might be due to the relatively fast adsorption of Li on graphene surfaces (Mechanism 3). Based on first principle density-functional theory calculations^{5,6}, Li atoms are capable of forming stable interactions with C atoms on a graphene plane. The results indicate that the Li-C bond in such a layer (without a functional group) would not result in an sp^2 to an sp^3 transition of carbon orbitals, but being more indicative of some ionic character for the covalent bond and with lithium acting as an electron acceptor in a bridging environment⁶. Energy calculations indicate the possible stability of such Li atom-adsorbed graphene layers and that the Li-adsorbed graphene layer can be spontaneously formed⁶. Adsorption of lithium atoms on graphene was also studied by others⁷⁻⁹. Pan *et al.*¹⁰ reported a high reversible capacity of 794-1054 mAh/g for heavily defected NGPs obtained by reduction of highly oxidized GO (Mechanism 4: defect-trapping). For small graphene sheets, Li_xC_6 (with $x = 1-4$) has been considered possible¹¹. The results of a preliminary study on the Li ion capturing mechanisms were reported elsewhere¹. A clear differentiation of the different contributions from individual mechanisms requires additional research, but we have herein observed that the specific surface areas of graphene sheets play a critical role in dictating the Li storage capacity at the cathode. As indicated in Fig. 2B, the higher the specific surface area, the greater the specific capacity of the various graphene-based cathodes (pristine graphene, graphene oxide,

graphene from graphite fibers, and thermally exfoliated graphite oxide). These measurements were motivated by the notion that graphene sheets have a high tendency to re-stack together due to van der Waals forces. Extrapolation of these data points to the theoretical surface area limit of single-layer graphene (2670 m²/g) indicates that graphene surfaces, as a cathode active material, are capable of storing up to 935 mAh/g provided that all the surfaces are accessible to the electrolyte.

References

1. Jang, B. Z., Liu, C. G., Neff, D., Yu, Z. N., Wang, M. C., Xiong, W. & Aruna, Z.. Graphene surface-enabled lithium ion-exchanging cells: next-generation high-power energy storage devices. *Nano Lett.* **11**, 3785-3791 (2011).
2. Le Gall, T. L., Reiman, K. H., Grossel, M. C. & Owen, J. R. Poly (2,5-dihydroxy-1,4-benzoquinone-3,6-methylene): a new organic polymer as positive electrode material for rechargeable lithium batteries. *J. Power Sources* **119**, 316–320 (2003).
3. Chen, H., Armand, M., Demailly, G., Dolhem, F., Poizot, P. & Tarascon, J. M. From biomass to a renewable Li_xC₆O₆ organic electrode for sustainable Li-ion batteries. *ChemSusChem* **1**, 348-355 (2008).
4. Lee, S. W., Yabuuchi, N., Gallant, B. M., Chen, S., Kim, B. S., Hammond, P. T. & Yang, S. H. High power lithium batteries from functionalized carbon nanotubes. *Nature Nanotech.* **5**, 531-537 (2010).
5. Khantha, M., Cordero, N. A., Molina, L. M., Alonso, J. A. & Girifalco, L. A. Interaction of lithium with graphene: An *ab initio* study. *Physical Review B* **70**, 125422-125429 (2004).
6. Medeiros, P. V C, de BritoMota, F., Mascarenhas, A. J. S. & de Castilho, C. M C. Adsorption of monovalent metal atoms on graphene: a theoretical approach. *Nanotechnology* **21**, 115701-115706 (2010).
7. Sato, K., Noguchi, M., Demachi, A., Oki, N. & Endo, M. A mechanism of lithium storage in disordered carbons. *Science* **264**, 556-558 (1994).
8. Dahn, J. R., Zheng, T., Liu, Y. H. & Xue, J. S. Mechanisms for lithium insertion in carbonaceous materials. *Science* **270**, 590-593 (1995).
9. Yoo, E., Kim, J., Hosona, E., Zhou, H., Kudo, T. & Honma, I. Large reversible Li storage of graphene nanosheet families for use in rechargeable lithium ion batteries. *Nano Lett.* **8**, 2277-2282 (2008).
10. Pan, D., Wang, S., Zhao, B., Wu, M., Zhang, H., Wang, Y. & Jiao, Z. Li storage properties of disordered graphene nanosheets. *Chem. Mater.* **21**, 3136–3142 (2009).
11. Gerouki, A., Goldner, M. A., Goldner, R. B., Hass, T. E., Liu, T. Y. & Slaven, S. Density of states calculations of small diameter single graphene sheets. *J. Electrochem. Soc.* **143**, L262-263 (1996).
12. Xue, R., Huang, H., Li, G. & Chen, L. Effects of cathode anode mass-ratio in lithium-ion secondary cells. *J. Power Sources* **55**, 111-114 (1995).